LASER REFLECTIONS FROM THE BEACON EXPLORER SATELLITES (U)
(Unclassified)

H. H. Plotkin

National Aeronautics and Space Administration
Goddard Space Flight Center
Greenbelt, Maryland

ABSTRACT
(Unclassified)

Two satellites have been supplied by the Goddard Space Flight Center with arrays of cube-corner reflectors, and have been used as orbiting targets for ruby laser radiation. The observed intensity of reflected radiation is in agreement with theory. Although the distribution of the reflected light is affected by target geometry and atmospheric fluctuations, qualitative agreement was found with calculations of velocity aberration due to the satellite's motion. The system has been used to determine satellite range.

1. INTRODUCTION

This paper is a preliminary report on a series of experiments now being performed as part of NASA's program in developing techniques for space communication, navigation, and tracking with laser beams. Although these objectives do not correspond to the primary aims of this Symposium, the techniques and some of the results may be very pertinent in discussing possible methods for identifying space objects.

Briefly, our objective was to place into orbit satellites with as large an effective retro-reflecting area as we could. From a ground station, we would then illuminate the satellite with a pulse of light. The reflected light would be detected photoelectrically and its time of flight measured to yield range. In a different mode of operation, not discussed in this paper, the reflected light can also be photographed against a star background to yield precise angular position. This appeared to be a worthwhile project from our point of view. First, it would constitute a precise tracking tool for geodetic purposes and orbit analysis; secondly, it would exercise many of the elements of an optical communication system: Laser transmitters of different types could be used as they were developed, receivers could be evaluated, means could be developed and checked for aiming very narrow beams of coherent light, and the attenuating and dispersive effects of atmospheric transmission could be studied.

That we succeeded in receiving laser light reflected from these satellites is illustrated in Figure 1. The upper oscilloscope trace is a sample of the transmitted light from a pulsed ruby laser, and the lower trace the received photoelectric signal. Each trace is swept at two microseconds per large division, but the initiation of the lower one has been delayed by about seven milliseconds to account for the time-of-flight. This paper will describe the experiment and some of its early results.

2. THE BEACON-EXPLORER SATELLITES

Two identical satellites, designated by NASA code S-66, were orbited: Explorer 22 was launched October 10, 1964 into an orbit with inclination 79.7°, apogee 1100 km, and perigee 939 km. Explorer 27 was launched April 29, 1965 into an orbit with inclination 41°, apogee 1,318 km, and perigee 939 km. By means of a permanent bar magnet, each satellite is constrained to orient itself along the lines of force of the earth's magnetic field: One end of the symmetry axis always points in the north-seeking direction (Figure 2). Since the magnetic dip angle is about 70° below horizontal near Washington, D. C., a special array of reflectors was mounted on this end (Figure 3) to provide a large effective retroreflecting area for ground stations in north temperate locations. Although the primary mission of the satellites was to study the density distribution of electrons in the Ionosphere (Reference 1), space and weight were made available for the reflecting structure (Additional design details are contained in Reference 2).

The array (Figure 4) consists of 360 cube corner prisms arranged over nine panels which form a truncated octagonal pyramid. At the base of the pyramid, the diameter of an inscribed circle is about 18 inches, and its height is about 10 inches. The individual prisms are of radiation-resistant fuzed quartz with aluminized reflecting surfaces, cut at the corners to yield hexagonal faces for optimum area usage. They are about one inch across flats.

A cube corner reflector has the property that each ray of light entering its aperture suffers three reflections and leaves in exactly the opposite direction from which it entered. An incident beam of parallel light retroreflected from the Beacon-Explorer array, however, will not remain perfectly collimated. The reflected light will diverge because of diffraction effects, non-orthogonality of the reflecting faces, and other optical imperfections. This spreading was measured in the laboratory by illuminating individual cubes and the entire satellite with collimated light, and then examining the reflected energy distribution in the far field. The gross character of the variation of intensity with angular displacement from the incident beam is shown in Figure 5.

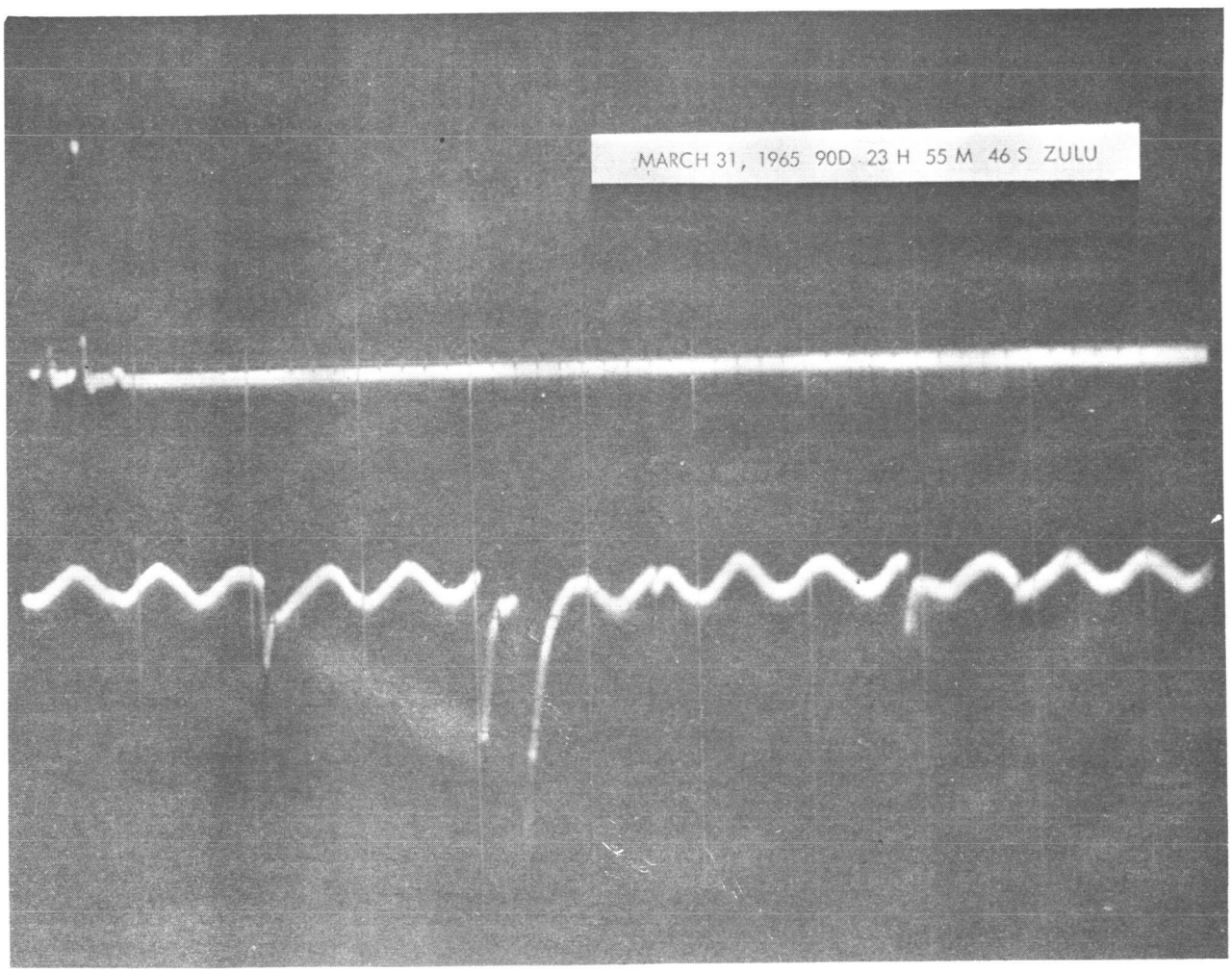

FIGURE 1. PHOTOELECTRIC DETECTION OF REFLECTED LASER RADIATION FROM SATELLITE EXPLORER 27. Upper trace shows two transmitted pulses, lower trace, delayed by about 7 milliseconds, shows received reflection of same two pulses. Ripple is instrumental in nature, and not significant.

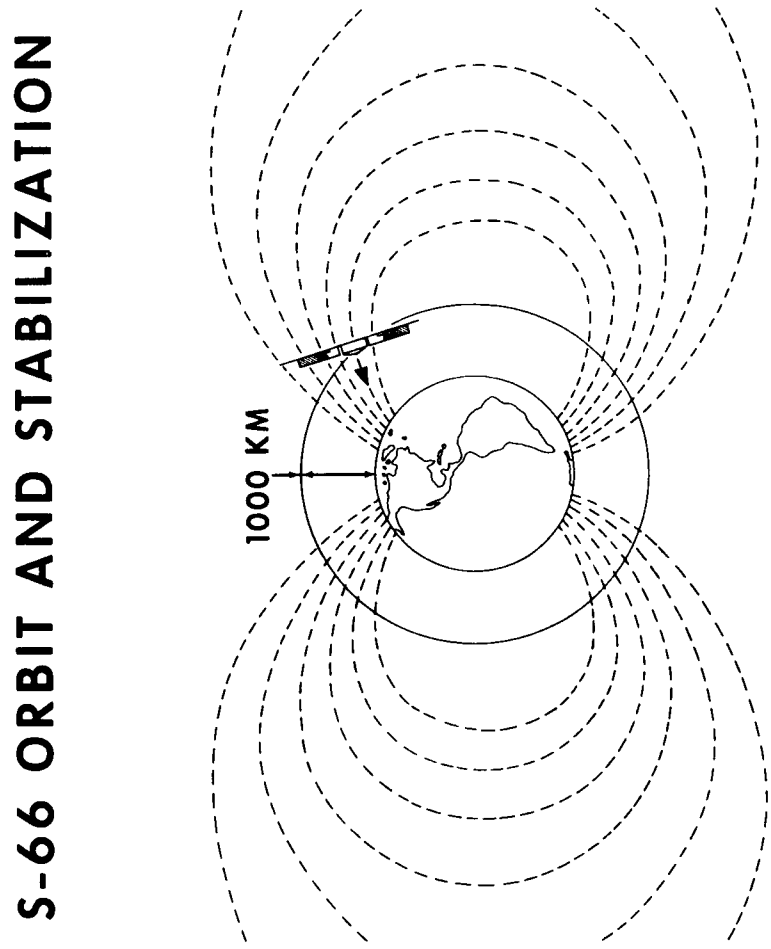

FIGURE 2. STABILIZATION OF BEACON-EXPLORER ATTITUDE BY EARTH'S MAGNETIC FIELD.

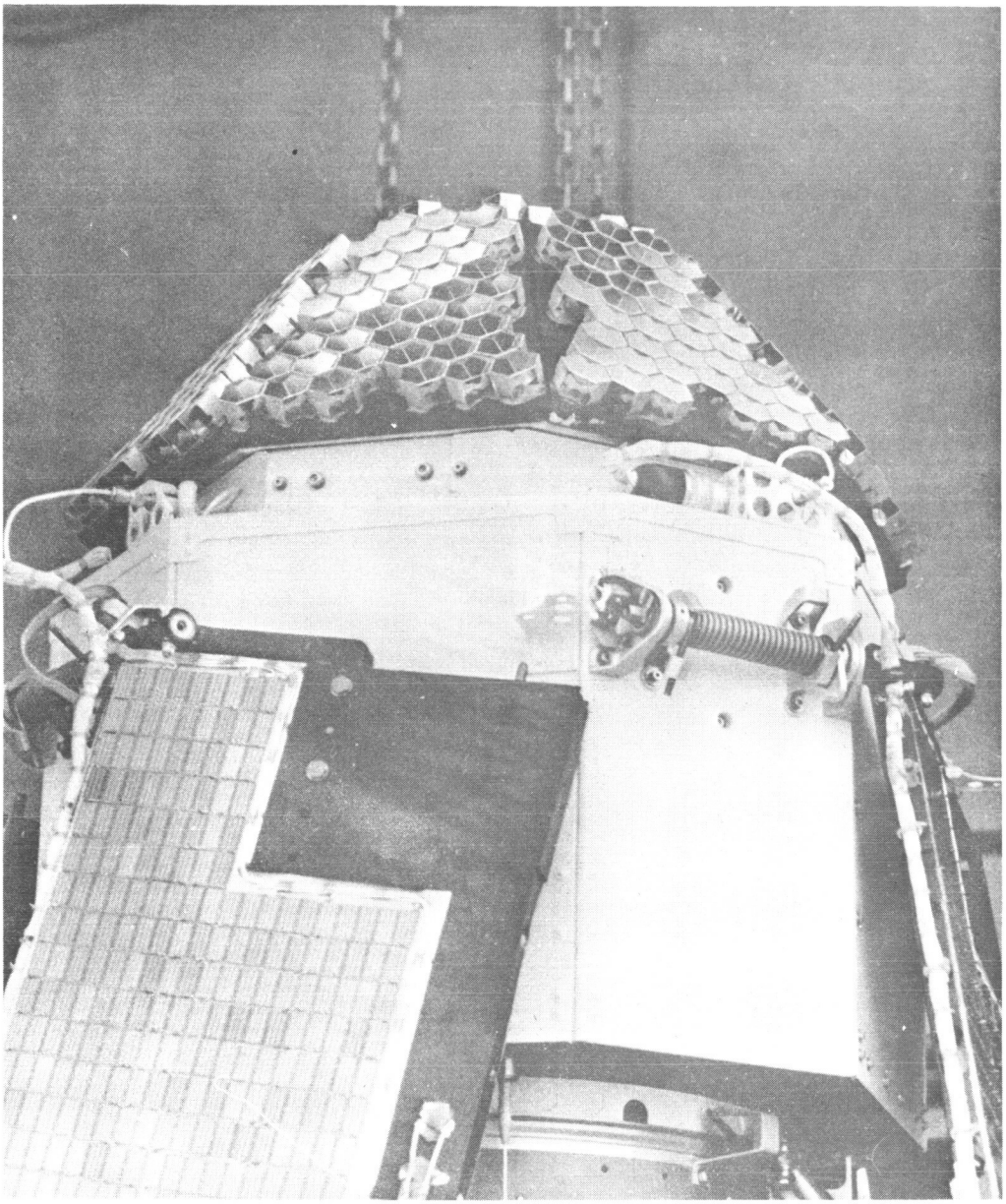

FIGURE 3. THE BEACON-EXPLORER-B SATELLITE (EXPLORER 22), WITH ARRAY OF CUBE-CORNER REFLECTORS ON NORTH-SEEKING END.

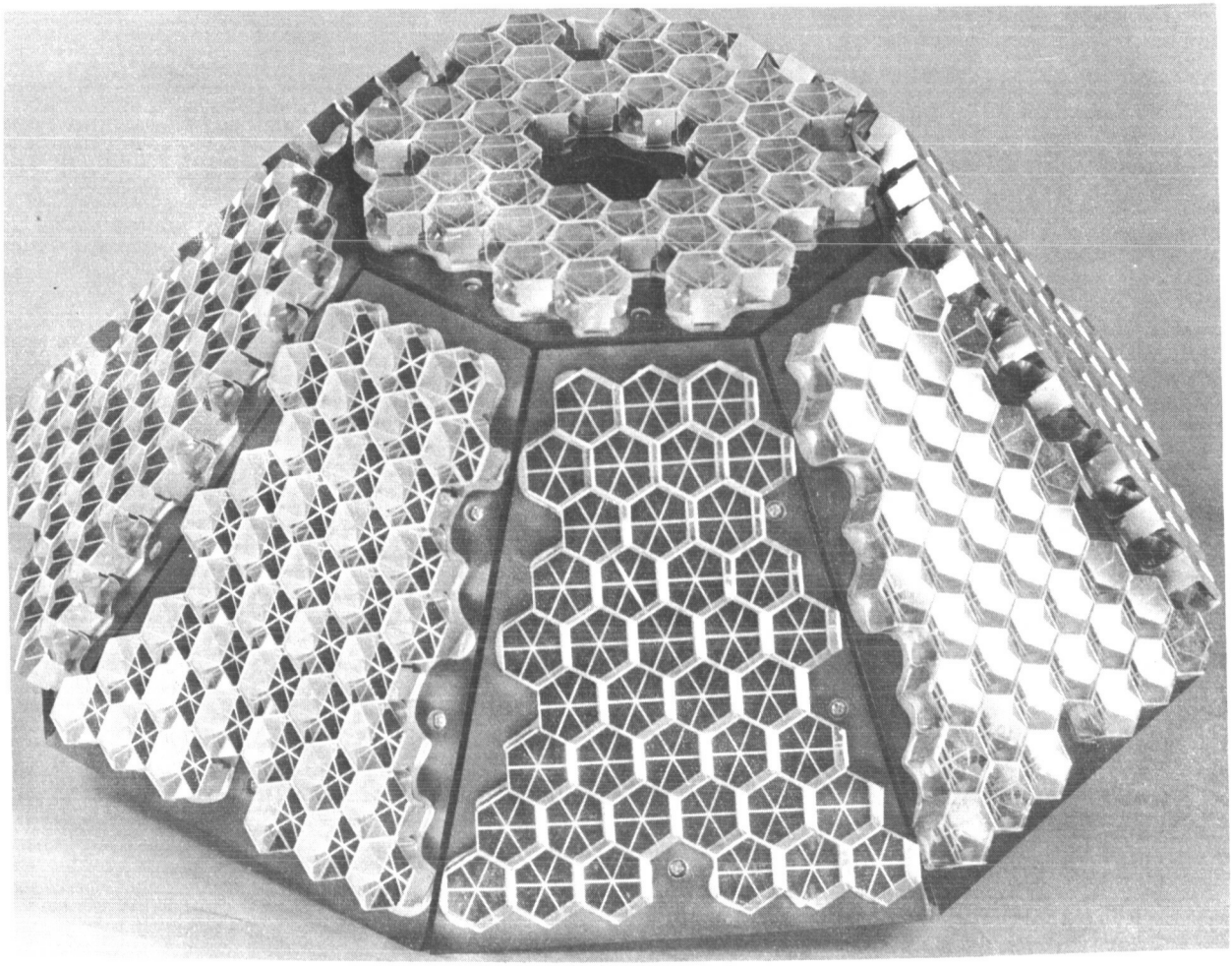

FIGURE 4. DETAILED PHOTOGRAPH OF ARRAY OF FUZED QUARTZ CUBE-CORNER RETRO-REFLECTORS.

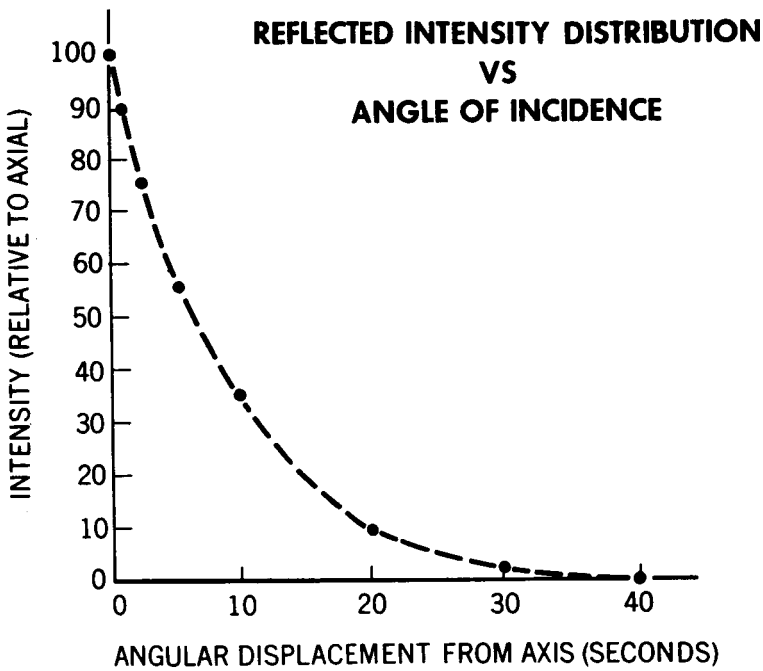

FIGURE 5. DISTRIBUTION OF ENERGY DENSITY IN THE LIGHT REFLECTED FROM THE SATELLITE ARRAY AS A FUNCTION OF ANGULAR DISPLACEMENT FROM THE AXIS, WHEN THE ARRAY IS ILLUMINATED BY A COLLIMATED BEAM PARALLEL TO THE AXIS.

Unfortunately this does not show the fine granular or mottled appearance observed when the reflectors were illuminated with laser light. When examined closely, the reflected light showed intricate patterns arising from diffraction at the prism apertures and at the intersections of the reflecting planes, and from interference between reflections from different prisms superimposed on one another. The detector aperture used to obtain Figure 5 subtended many of these fluctuations, and so it is useful as a qualitative indication of the smoothed overall distribution.

The effective reflecting area of the satellites as the line of sight makes different angles with respect to the symmetry axis, was also measured in the laboratory and is shown in Figure 6. This is the equivalent area of a plane 100% reflecting mirror oriented perpendicularly to the incident beam so as to reflect light back to the source. The two cases in the figure refer to incident beams approaching across one of the octagon corners or across one of the flats, respectively, and show that it is only the angle which the beam makes with the axis which is significant. In qualitative calculations of signal intensity, a value of $80cm^2$ is used for the area, and the figure shows that it actually remains above this value out to angles as large as 70 degrees from the axis, which corresponds to a large portion of every pass over a station.

3. THE GROUND STATION

The transmitter-receiver used for S-66 is illustrated in Figure 7. A Nike-Ajax radar pedestal was modified for this purpose: After removing the dish and radar electronics, a 16-inch aperture, 300-inch focal length cassegrain telescope was mounted on the central support disc. A second small cylinder seen below the disc in the figure is part of the ruby laser transmitter.

The laser used a 6-1/2 inch ruby rod, 3/8 inch in diameter, and an FX-55 flash lamp in a 4-inch diameter cylindrical reflecting cavity. Both the ruby and lamp were cooled with purified water. It was "Q-switched" with a total-internal-reflection prism rotating at 24,000 rpm, but exhibited multiple spiking even when operating under optimum conditions. Typically, when the lamp was energized with 1200 joules, two or three spikes were produced in a single burst, having a total output energy of 0.3 joules, each pulse being about 50 nanoseconds in duration and pulse separated by 500 nsec. The transmitter was flashed at a rate of one pps. An optical system collimated the 6943 Angstrom output radiation into a fairly uniform beam contained within a cone of 1.2×10^{-3} radian, full angle.

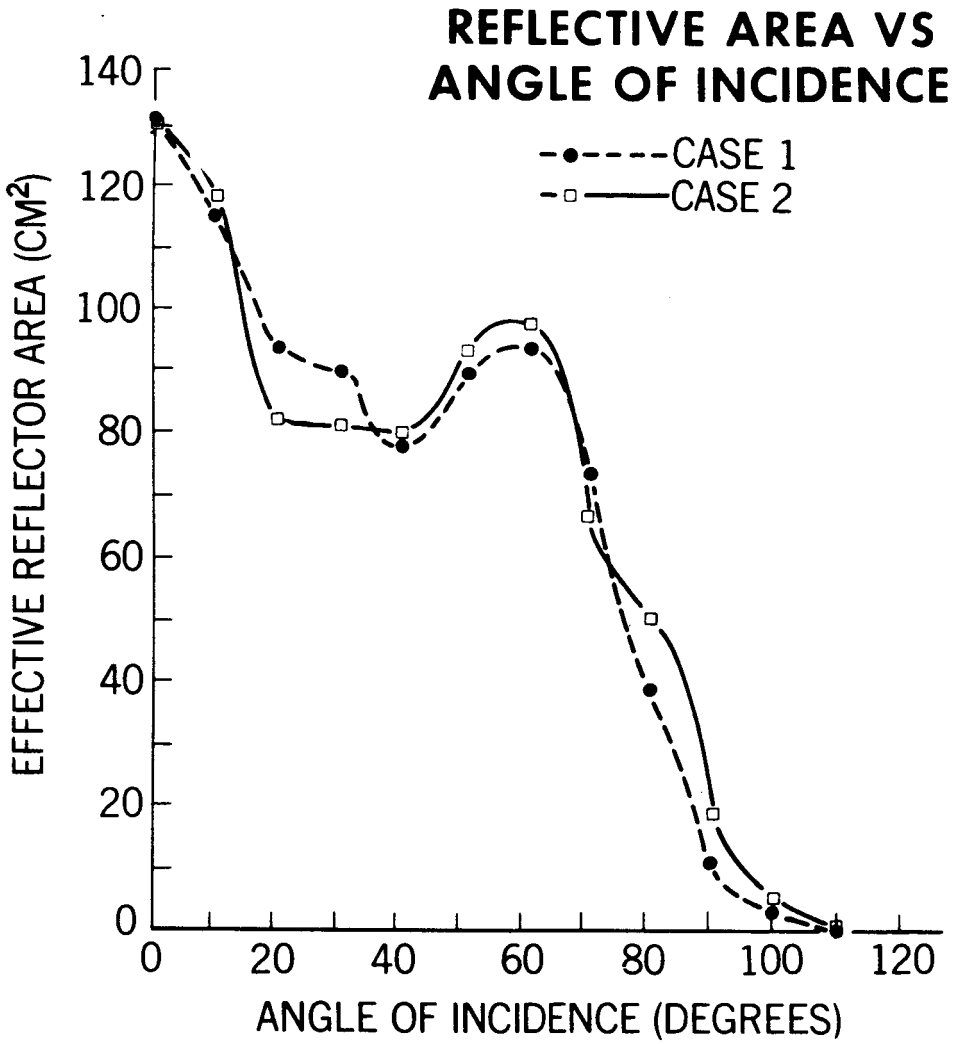

FIGURE 6. VARIATION OF EQUIVALENT REFLECTING AREA OF SATELLITE ARRAY WITH ANGLE BETWEEN INCIDENT BEAM AND SYMMETRY AXIS.

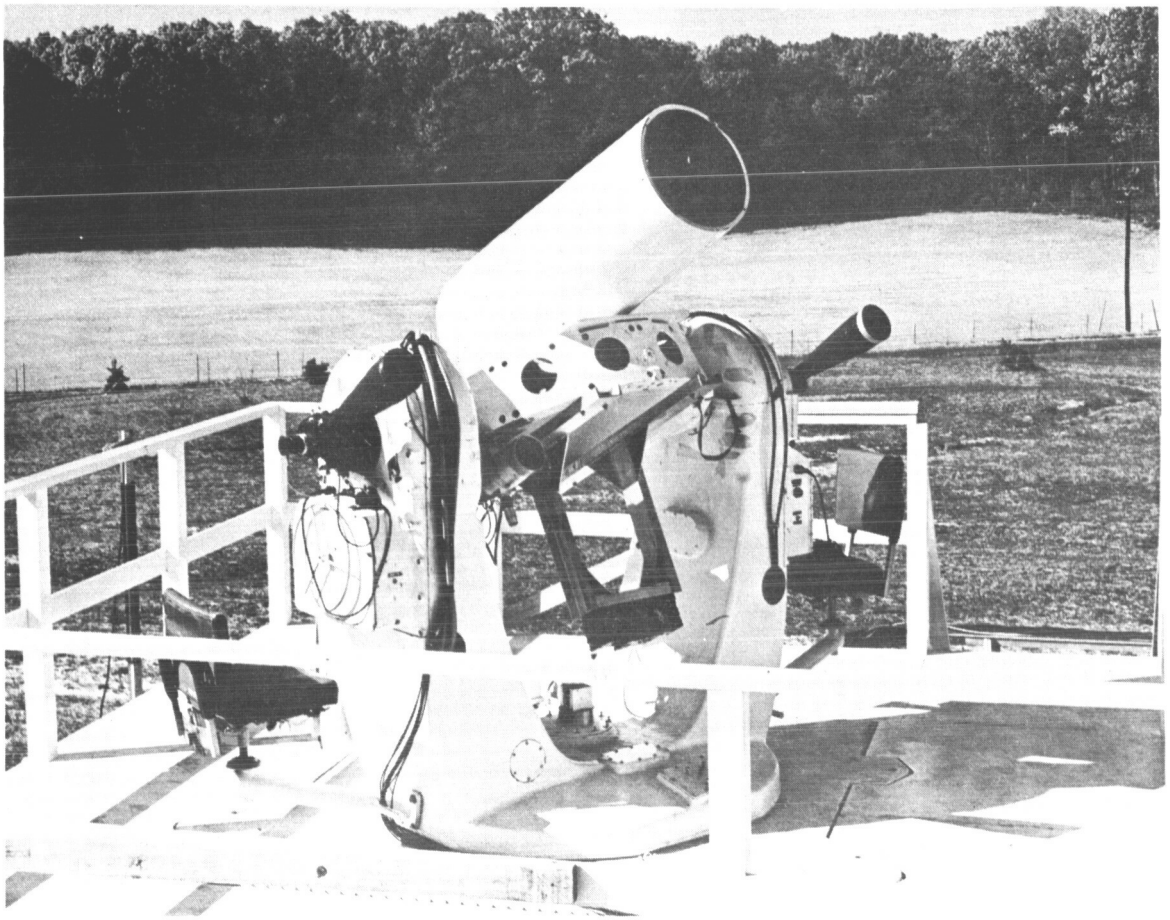

FIGURE 7. TRANSMITTING LASER AND RECEIVING TELESCOPE, MOUNTED ON A MODIFIED NIKE-AJAX RADAR PEDESTAL.

During a pass, the mount which is equipped with digital encoders is directed toward the expected position of the satellite by a programmer fed with punched paper tape. Usually, the accuracy of the mount and orbital predictions enables us to point to within one or two milliradians. Operators looking through auxiliary viewing scopes can then see the satellite in reflected sunlight and can make small corrections to keep the satellite image on cross hairs so that it is illuminated by the transmitted laser beam. Since the transmitter and receiver are carefully boresighted together, the satellite is then also in the receiver field of view. The receiver used a 9558A photomultiplier together with a filter having a 10 Angstrom band-pass.

In order to display the received signal and to record data, the equipment schematically shown in Figure 8 was used. A photodiode picked off a small portion of each transmitted pulse, which was then used for several purposes. First, it was displayed on one trace of a double beam oscilloscope as a record of the transmitted radiation. Second, it started a Time-Interval unit which would be necessary for measuring range. Third, it started a range-gate generator, which was programmed with the expected time-of-flight for the round trip to the satellite and back. Ten microseconds before the reflected signal was expected, the output of the range-gate generator triggered the sweep on the second trace of the oscilloscope, and de-inhibited the "stop" circuit of the Time-Interval unit, which had been protected against noise pulses up to that time.

4. SIGNAL INTENSITY

The reflected energy collected by the receiver in each pulse is given by an equation of the form

$$\text{Signal} = \frac{E_t A_c A_t \tau^2 \alpha \gamma \Delta}{\pi^2 \theta_t^2 \theta_c^2 R^4}$$

E_t, the transmitted energy in a single pulse, was taken as 0.1 joule in this conservative estimate.

A_c is the target retroreflecting area and α is its reflectivity. Their product has already been illustrated as a function of angle of incidence in Figure 6. $A_c\alpha$ is assumed to be $80 cm^2$.

A_t is the 16-inch telescope receiving aperture, $0.114 m^2$.

τ^2 is the two-way atmospheric transmission, assumed to be 0.5 at this wavelength and for typical elevation angles.

γ is the receiving telescope transmission, 0.8.

Δ is the filter pass-band transmission, 0.5.

θ_t is the half-angle of the divergence cone of the transmitted beam, 6×10^{-4} radians. We have assumed, for this calculation, that all the energy is uniformly spread in this cone.

θ_c is the half-angle of the divergence cone of the reflected beam. From Figure 5, we have assumed a value of 5×10^{-5} radians, and again consider all the energy uniform within the cone.

R is the satellite range, assumed to be 1100 km. for this calculation.

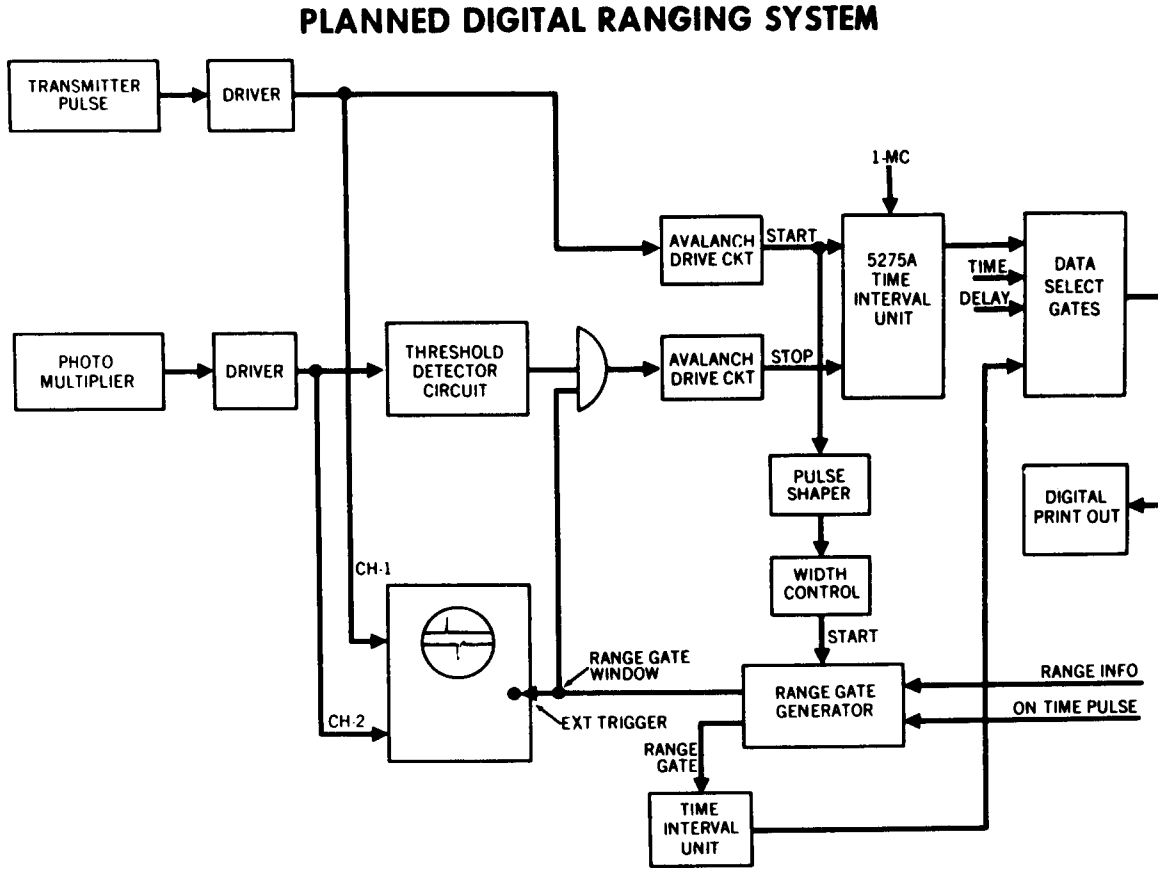

FIGURE 8. BLOCK DIAGRAM OF ELECTRONIC EQUIPMENT FOR SIGNAL DISPLAY AND SATELLITE RANGE MEASUREMENT. Not shown is movie camera to photograph oscilloscope.

The values listed above lead to a signal of 1.4×10^{-15} joules, or about 5000 photons per pulse. An S-20 photocathode surface, such as in our 9558A photomultiplier, has a quantum efficiency of about 2%, so we may expect about 100 photoelectrons to be released in each pulse. These are then amplified by a factor of about 10^6 in the multiplication structure of the tube, giving rise to pulses of about 1.6×10^{-11} coulomb. This charge would be expected to produce pulses of about 0.3 volts across the load capacitance of our detector. Actually we observed spikes as large as 0.1 volt. (The sensitivity of the lower trace in Figure 1 is 20 millivolt/cm.)

We consider the agreement reasonably good in view of some of the vague assumptions that have been made in the calculation. More careful estimates and measurements will be made during the course of this program.

Signals could be received and satellite ranges determined for many points during the pass of a satellite over the station. Figure 9 is a portion of a good pass during which over 80% of the transmitted pulses yielded range measurements.

5. EFFECTS OF VELOCITY ABERRATION

Because of the relative velocity of the satellite with respect to the transmitter on the ground, the reflected light from the on-board retrodirectors does not fall back onto the transmitter but suffers a displacement. This has been called, at various times, the Bradley effect, the transit-time effect, or velocity aberration. To observe this effect, a second identical receiver was installed at the ground station. The two receivers were displaced from each other by 85 feet along a north-south line. The laser transmitter was mounted alongside the receiver on the south mount, and boresighted to it, while the receiver on the north mount was slaved to the south, so that all three optical systems always pointed in the same direction.

Each of the receivers will thus find itself displaced by varying amounts from the center of the return spot, and this will affect the received intensity. Although a great deal of scatter was observed, we found at least qualitative agreement with theory. We shall estimate the magnitude of this effect by considering the apparent difference in the direction of a ray of light as observed from the ground and from the satellite.

In Figure 10, the satellite velocity is taken parallel to the x-axis on the ground. Another parallel set of coordinates is assumed to be moving with the satellite. The incident beam of light is a vector whose tip is instantaneously at position (x, y) as seen from the ground, and at (x^1, y^1) as seen from the moving system. The velocity vector of the light beam then is $(\dot{x}, \dot{y})$ and $(\dot{x}^1, \dot{y}^1)$ respectively in the two systems. Special relativity provides the necessary transformations.

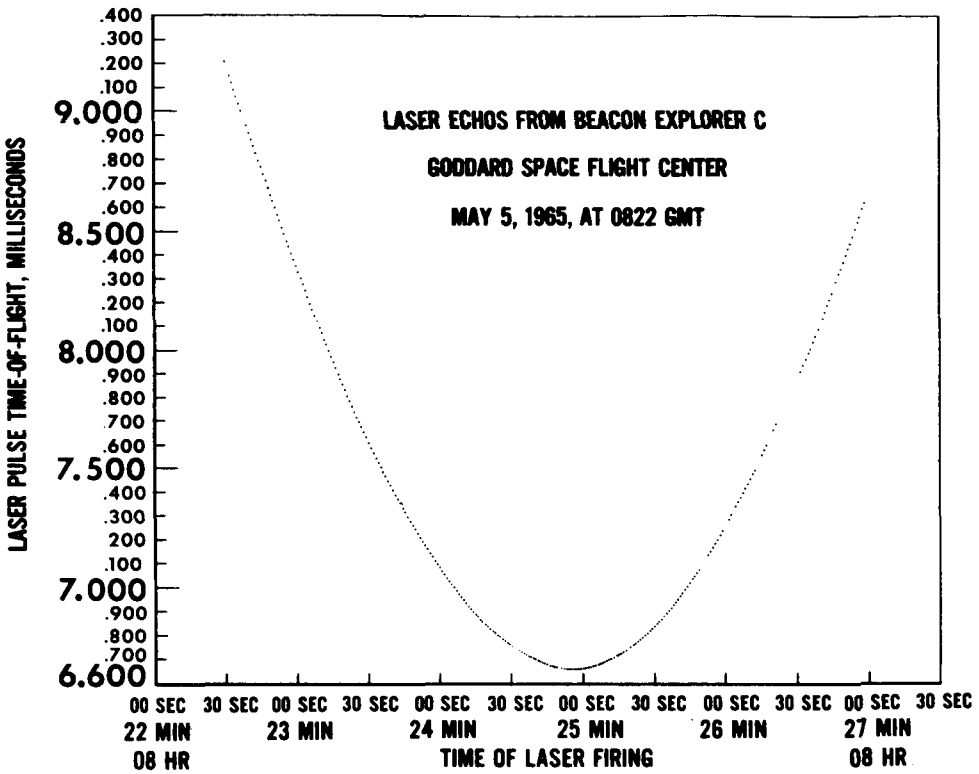

RANGE DETERMINATIONS ON BEACON EXPLORER C (EXPLORER 27) DURING A PASS OVER GODDARD ON MAY 5, 1965. EACH POINT REPRESENTS A LASER FLASH, RECEPTION OF AN ECHO, AND DETERMINATION OF RANGE FROM THE ROUND TRIP TIME OF FLIGHT. LASER WAS FLASHED AT THE RATE OF ONCE PER SECOND.

FIGURE 9. MEASUREMENTS OF RANGE VS. TIME ON EXPLORER 27.

$$\left.\begin{aligned} x' &= \frac{x - vt}{\sqrt{1-\beta^2}} \quad , \quad \beta = \frac{v}{c} \\ y' &= y \\ t' &= \frac{t - \beta\frac{x}{c}}{\sqrt{1-\beta^2}} \end{aligned}\right\} \tag{1}$$

$$\left.\begin{aligned} dx' &= \frac{dx - v\,dt}{\sqrt{1-\beta^2}} \\ dy' &= dy \\ dt' &= \frac{dt - \beta\frac{dx}{c}}{\sqrt{1-\beta^2}} \end{aligned}\right\} \tag{2}$$

The components of the velocity of the ray of light are then

$$\left.\begin{aligned} c_{x'} &= \frac{dx'}{dt'} = \frac{c_x - v}{1 - \beta\frac{c_x}{c}} \\ c_{y'} &= \frac{dy'}{dt'} = \frac{c_y\sqrt{1-\beta^2}}{1 - \beta\frac{c_x}{c}} \end{aligned}\right\} \tag{3}$$

From the ground, the beam appeared to have the angle θ, where

$$\tan\theta = \frac{c_x}{c_y} \tag{4}$$

but in the moving system, the angle is given by

$$\tan\theta' = \frac{c_{x'}}{c_{y'}} = \frac{c_x - v}{c_y\sqrt{1-\beta^2}} \tag{5}$$

At this point, it is apparent that the difference between a classical and a relativistic calculation of this effect cannot be significant. The velocity of the satellite in its orbit is about 7.5 km/sec. This gives β a value of 2.5×10^{-5} and β^2 a value of 6×10^{-10}. Clearly, it should be ignored in eq. (5), and the result becomes identical to that predicted classically.

The action of the retroreflector is to reverse the direction of the beam as it is observed in the satellite's coordinates, i.e., each of the primed components is reversed. (Notice we have dropped the relativistic affectation.)

$$\begin{aligned} c_{x'} &\longrightarrow -c_{x'} = -c_x + v \\ c_{y'} &\longrightarrow -c_{y'} = -c_y \end{aligned} \tag{6}$$

In returning to the earth, we must transform the ray once more back to the ground coordinates, because the ground observer will automatically add the satellite's velocity to whatever vector velocity was measured on the satellite.

$$\begin{aligned} c_{x''} &= -c_{x'} + v = -c_x + 2v \\ c_{y''} &= -c_{y'} = -c_y \end{aligned} \tag{7}$$

The angle at which the beam approaches the ground is given by

$$\tan\theta'' = \frac{c_{x''}}{c_{y''}} = \frac{-c_x + 2v}{-c_y} = \frac{-c\sin\theta + 2v}{-c\cos\theta} \tag{8}$$

$$\tan\theta'' = \tan\theta - \frac{2v}{c\cos\theta} \tag{9}$$

Figure 11 shows that eq. (9) can be given a simple geometrical interpretation. The distance δ is the displacement from the transmitter of the spot produced by the reflected ray as it intersects the x-axis. From the two triangles it can be seen that

$$\begin{aligned} \delta &= R\cos\theta\tan\theta'' - R\sin\theta = R\cos\theta(\tan\theta'' - \tan\theta) \\ \delta &= 2\tfrac{v}{c}R \end{aligned} \tag{10}$$

Our coordinate system was deliberately chosen with the satellite velocity parallel to the x-axis, and with the line-of-sight in the x-y plane. In general, we can say that $\vec{\delta}$ is a vector parallel to $\vec{v}$, and with a magnitude given by (10). The general situation is pictured in Figure 12, The transmitter is located at S, which is the location of our south mount. There are receivers both at S and at N, the north telescope. The transmitted beam travels along vector $\vec{R}$, and the reflected beam passes through the tip of the vector $\vec{\delta}$, drawn as originating from S and parallel to $\vec{v}$. The vector $\vec{b}$ is the position of the second receiver relative to the transmitter.

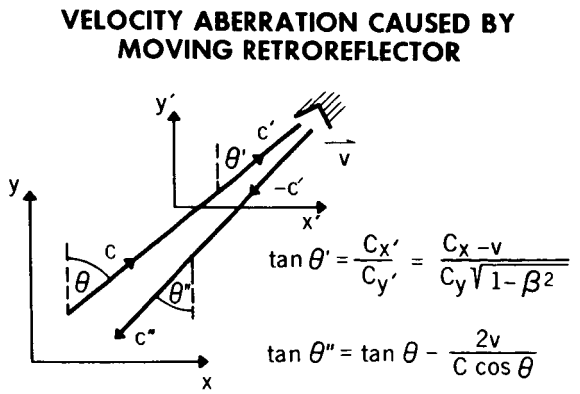

FIGURE 10. DERIVATION OF ANGULAR DISPLACEMENT OF REFLECTED BEAM DUE TO SATELLITE MOTION.

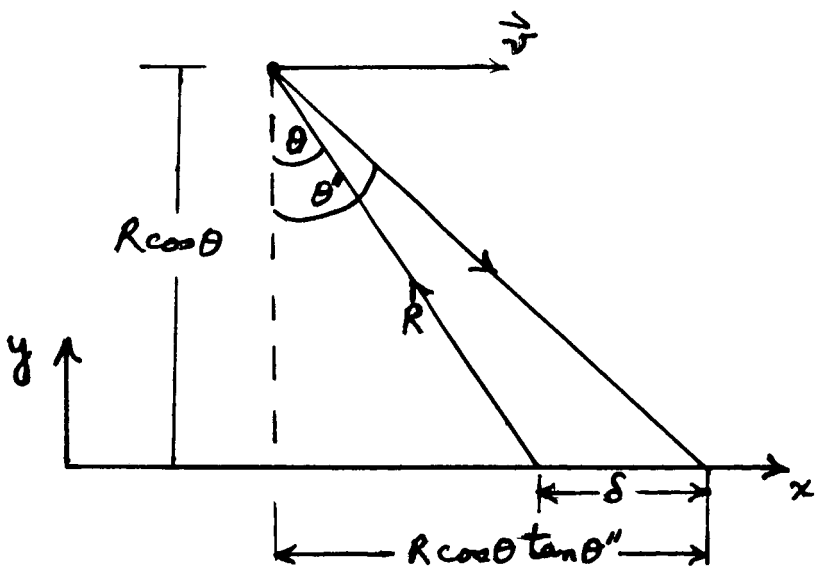

FIGURE 11. VELOCITY ABERRATION. Geometric relations.

We wish to perform the following calculation: If we can find the angular displacement of each of the receivers from the center of the reflected ray, then the intensity of the signal received at each telescope could be compared with the angular intensity distribution of the reflected light from the satellite, as measured with collimated light in the laboratory (see Figure 5). These results would then be expected to be consistent with our interpretation of the velocity aberration.

The angular displacement of S from the center of the beam is the component of $\vec{\delta}$ perpendicular to $\vec{R}$, divided by $|R|$. To find this, we write

$$\vec{q}_0 = \frac{\vec{R} \times \vec{\delta}}{|\vec{R} \times \vec{\delta}|} \tag{11}$$

which is a unit vector perpendicular to the plane of $\vec{R}$ and $\vec{v}$. Next,

$$\vec{\omega}_0 = \frac{\vec{q}_0 \times \vec{R}}{|\vec{q}_0 \times \vec{R}|} = \frac{1}{R}(\vec{q}_0 \times \vec{R}) \tag{12}$$

is a unit vector in the plane of $\vec{R}$ and $\vec{\delta}$, but perpendicular to $\vec{R}$. The component of $\vec{\delta}$ perpendicular to $\vec{R}$ is now simply

$$\delta_\perp = \vec{\delta} \cdot \vec{\omega}_0 \tag{13}$$

Calculating this in detail is not quite so simple. We have, putting (11) into (12),

$$\vec{\omega}_0 = \frac{(\vec{R} \times \vec{\delta}) \times \vec{R}}{R|\vec{R} \times \vec{\delta}|} \tag{14}$$

Use the vector identity

$$\vec{a} \times (\vec{b} \times \vec{c}) = \vec{b}(\vec{a} \cdot \vec{c}) - \vec{c}(\vec{a} \cdot \vec{b})$$

(14) then becomes

$$\vec{\omega}_0 = \frac{1}{R|\vec{R} \times \vec{\delta}|}\left[\vec{R}(\vec{R} \cdot \vec{\delta}) - \vec{\delta}(\vec{R} \cdot \vec{R})\right]$$

$$\delta_\perp = \frac{(\vec{R} \cdot \vec{\delta})^2 - \delta^2 R^2}{R|\vec{R} \times \vec{\delta}|} \tag{15}$$

and its angular displacement from the center of the return beam is

$$\alpha_s = \frac{\delta_\perp}{R} = \frac{(\vec{R} \cdot \vec{\delta})^2 - \delta^2 R^2}{R^2|\vec{R} \times \vec{\delta}|} \tag{16}$$

Similarly, to find the angular displacement of the second receiver from the center of the reflected ray, we put

$$\vec{\gamma} = \vec{\delta} - \vec{\ell} \tag{17}$$

By following the steps leading to (16), we would find that the angular displacement of the second receiver is

$$\alpha_N = \frac{\gamma_\perp}{R} = \frac{(\vec{R}\cdot\vec{\gamma})^2 - \gamma^2 R^2}{R^2\,|\vec{R}\times\vec{\gamma}|} \tag{18}$$

In principle, (16) and (18) should be sufficient to allow us to verify that the relative intensities observed at our north and south mounts are consistent with the velocity aberration effect.

We shall apply some simplifying assumptions to evaluate (16) and (18) for the BE-C and BE-B passes of May 10, 1965. A Cartesian coordinate system is set up with S as origin, the $\vec{\imath}$ x-axis in the horizontal north direction, the $\vec{\jmath}$ y-axis horizontally to the west (to maintain a right-hand character), and the $\vec{k}$ z-axis vertically upward. In terms of the satellite's instantaneous range R, azimuth φ, and zenith angle ψ:

$$\begin{aligned} R_x &= R \sin\psi \cos\varphi \\ R_y &= R \sin\psi \sin\varphi \\ R_z &= R \cos\psi \end{aligned} \tag{19}$$

The BE-C pass of May 10, 1965 is illustrated in polar coordinates in Figure 13. We can simplify our calculation, without introducing too great an error, if we assume that the satellite velocity during the pass is constant at 7.3 km/sec., in a west-to-east direction, and parallel to the x-y plane, i.e.

$$\begin{aligned} \vec{\delta} &= -\vec{\jmath}\,|\delta| \\ \vec{R}\times\vec{\delta} &= R_z\delta\vec{\imath} - R_x\delta\vec{k} \\ |\vec{R}\times\vec{\delta}| &= \delta\left[R_x^2 + R_z^2\right]^{1/2} \end{aligned} \tag{20}$$

(16) then becomes

$$\alpha_s = \frac{R_y^2\delta^2 - R^2\delta^2}{R^2\delta\left[R_x^2 + R_z^2\right]^{1/2}} = \frac{\delta}{R^2}\,\frac{R_y^2 - R^2}{\left[R^2 - R_y^2\right]^{1/2}} = \frac{\delta}{R^2}\left[R^2 - R_y^2\right]^{1/2}$$

If we insert the value of δ from (10), we obtain

$$\alpha_s = 2\beta\left[1 - \sin^2\psi\sin^2\varphi\right]^{1/2} \tag{21}$$

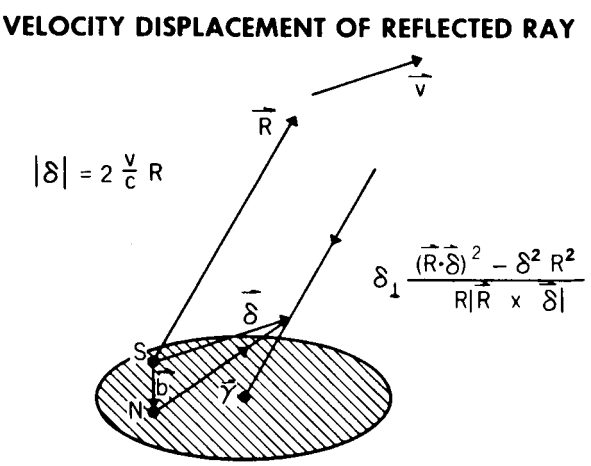

FIGURE 12. VELOCITY ABERRATION - VECTOR RELATIONSHIPS

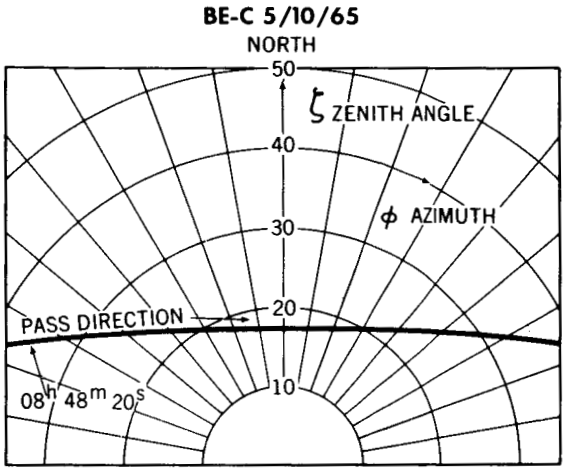

FIGURE 13. POLAR PLOT OF VISIBLE PORTION OF PASS OF EXPLORER 27 OVER GODDARD, ON THE MORNING OF MAY 10, 1965.

In this example, the vector $\vec{b}$ is the displacement of the north mount from the south

$$\vec{b} = \vec{\imath}\, b \tag{22}$$

The vector $\vec{\gamma}$ is now

$$\vec{\gamma} = \vec{\delta} - \vec{b} = -b\vec{\imath} - \delta\vec{\jmath} \tag{23}$$

To evaluate α_N,

$$\vec{R} \times \vec{\gamma} = R_z \delta \vec{\imath} - R_z b \vec{\jmath} + (R_y b - R_x \delta)\vec{k}$$

$$|\vec{R} \times \vec{\gamma}| = \left[R_z^2\delta^2 + R_z^2 b^2 + R_y^2 b^2 + R_x^2 \delta^2 - 2R_x R_y b\delta\right]^{1/2}$$

$$= \left[\delta^2(R_x^2 + R_z^2) + b^2(R_y^2 + R_z^2) - 2R_x R_y b\delta\right]^{1/2}$$

(18) becomes

$$\alpha_N = \frac{(-R_x b - R_y \delta)^2 - R^2(b^2 + \delta^2)}{R^2\left[\delta^2(R^2 - R_y^2) + b^2(R^2 - R_x^2) - 2R_x R_y b\delta\right]^{1/2}}$$

$$= \frac{1}{R^2}\left[R^2(b^2 + \delta^2) - (R_x b + R_y \delta)^2\right]^{1/2}$$

$$= \frac{1}{R^2}\left[R^2(b^2 + 4\beta^2 R^2) - (Rb\sin\zeta\cos\varphi + 2R^2\beta\sin\zeta\sin\varphi^2\right]^{1/2}$$

$$\alpha_N = \left[\left(\frac{b^2}{R^2} + 4\beta^2\right) - \left(\frac{b}{R}\sin\zeta\cos\varphi + 2\beta\sin\zeta\sin\varphi\right)^2\right]^{1/2} \tag{24}$$

(21) and (24) are the equations needed to analyze the BE-C pass.

The appearance of typical signals received simultaneously at the two receivers during the pass is shown in Figure 14. Each of the dots in the range vs. time plot of Figure 15 was derived from an oscilloscope record of this type. When the ratio of the intensities of signals in the two receivers is compared with the intensity ratios we might expect from the displacements in equations (21) and (24), we find a plot as in Figure 16. Qualitatively, at least, we can see that the intensity at the south mount is generally larger than at the north mount, as would be expected.

Similarly, the BE-B pass of May 10, 1965 is plotted on polar coordinates in Figure 17. For simplicity, this time we will assume that the velocity vector is horizontal and in the south-to-north direction

$$\vec{\delta} = \delta\vec{\imath} \tag{25}$$

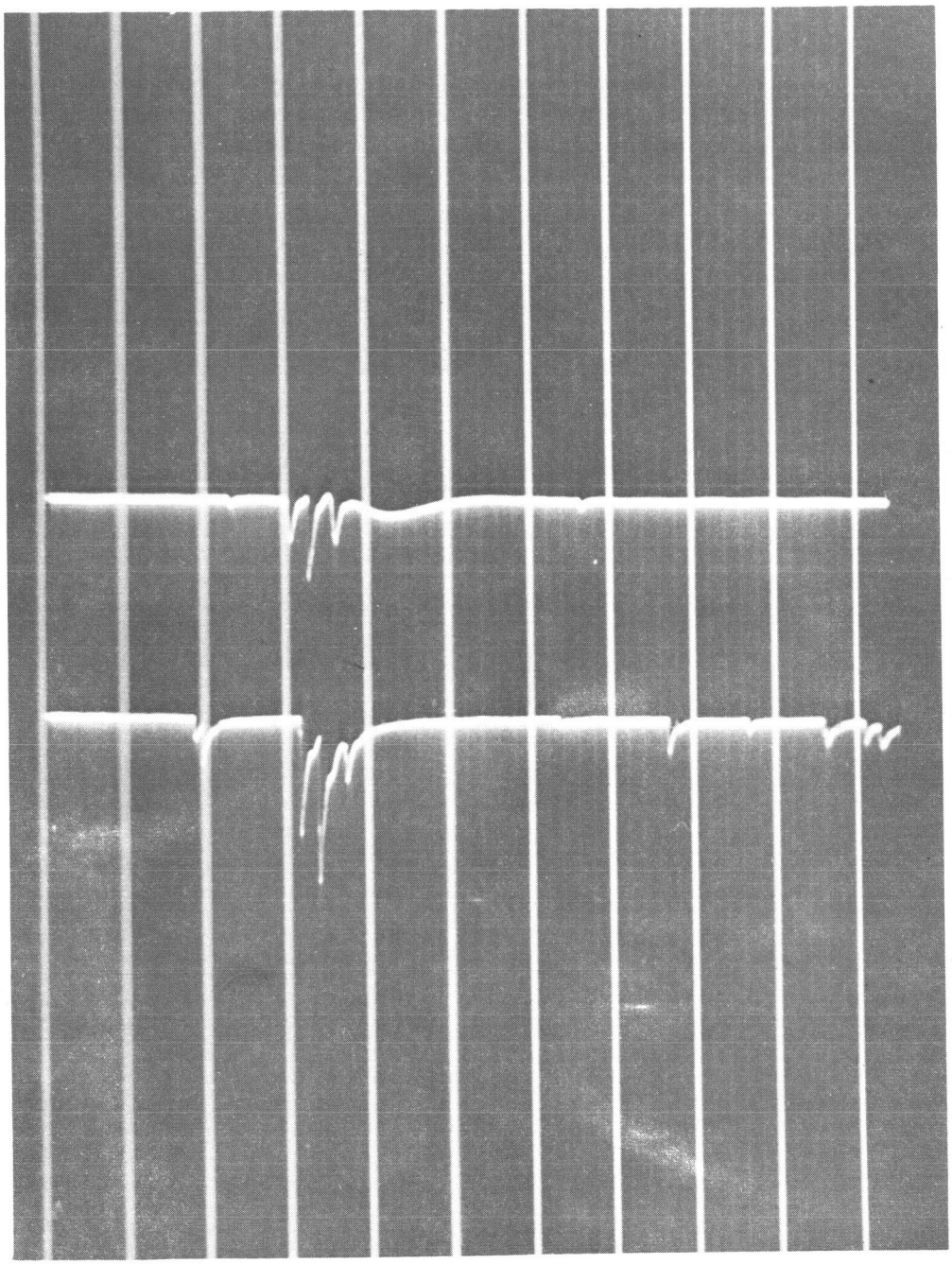

FIGURE 14. LASER REFLECTION SIGNALS FROM EXPLORER 27 RECEIVED SIMULTANEOUSLY AT RECEIVERS SEPARATED BY 85 FT. Transmitter was on same mount as South receiver (bottom trace). Sweep speed is 2 microseconds per large division.

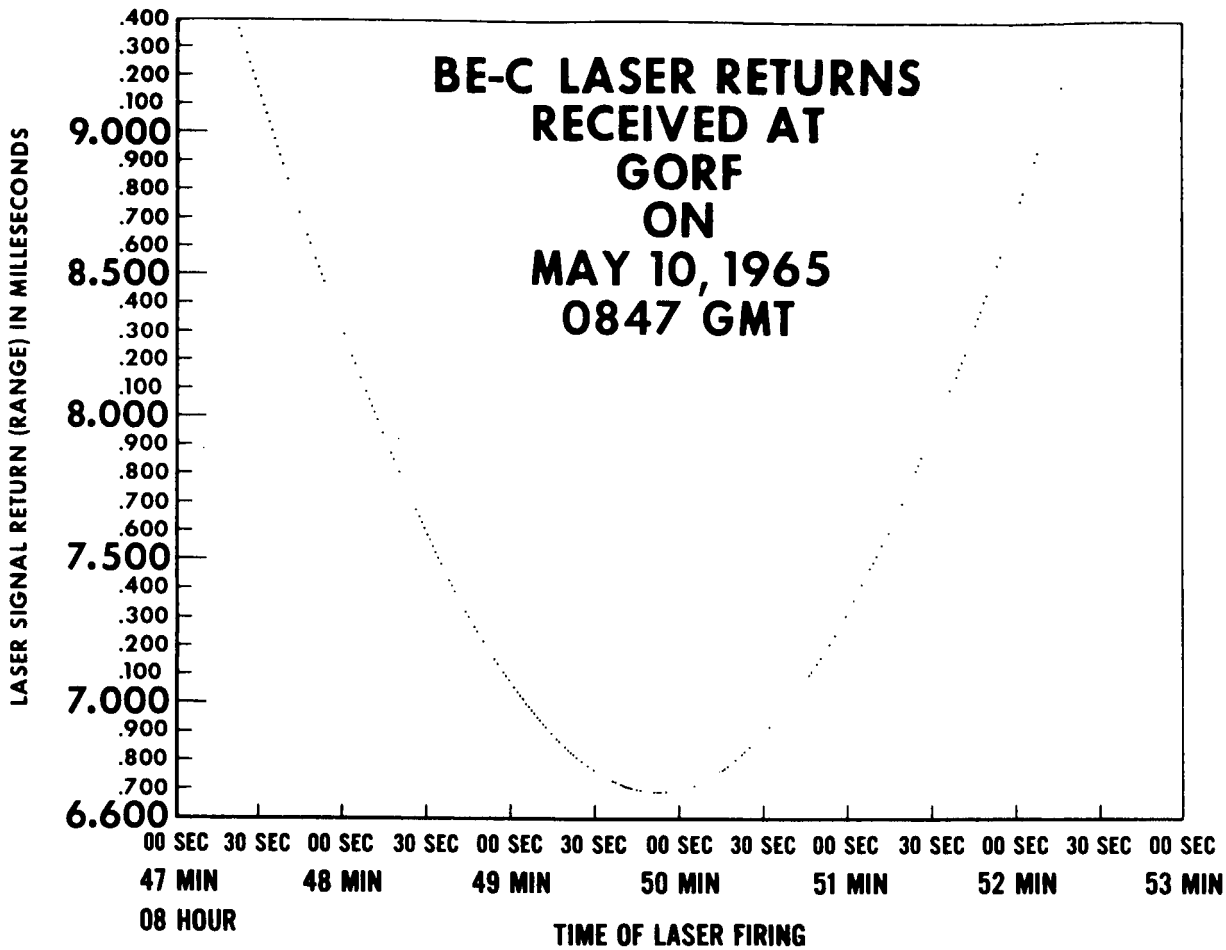

FIGURE 15. RANGE OF EXPLORER 27 DETERMINED BY LASER PULSE TIME-OF-FLIGHT DURING PASS OVER GODDARD OPTICAL RESEARCH FACILITY.

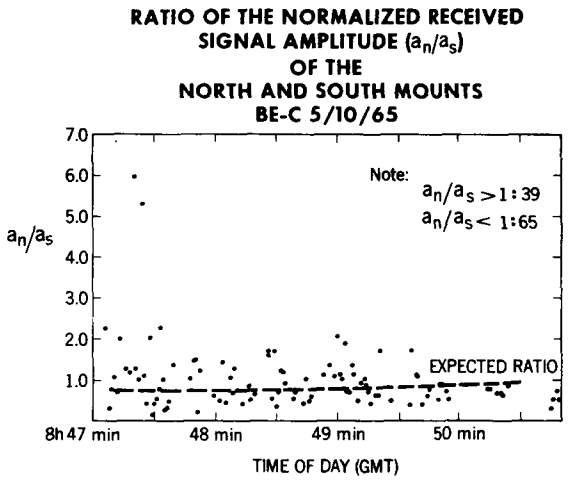

FIGURE 16. RATIO OF SIGNAL AMPLITUDE AT NORTH RECEIVER, a_n TO SIGNAL AT SOUTH RECEIVER a_s, FOR EACH LASER PULSE REFLECTION.

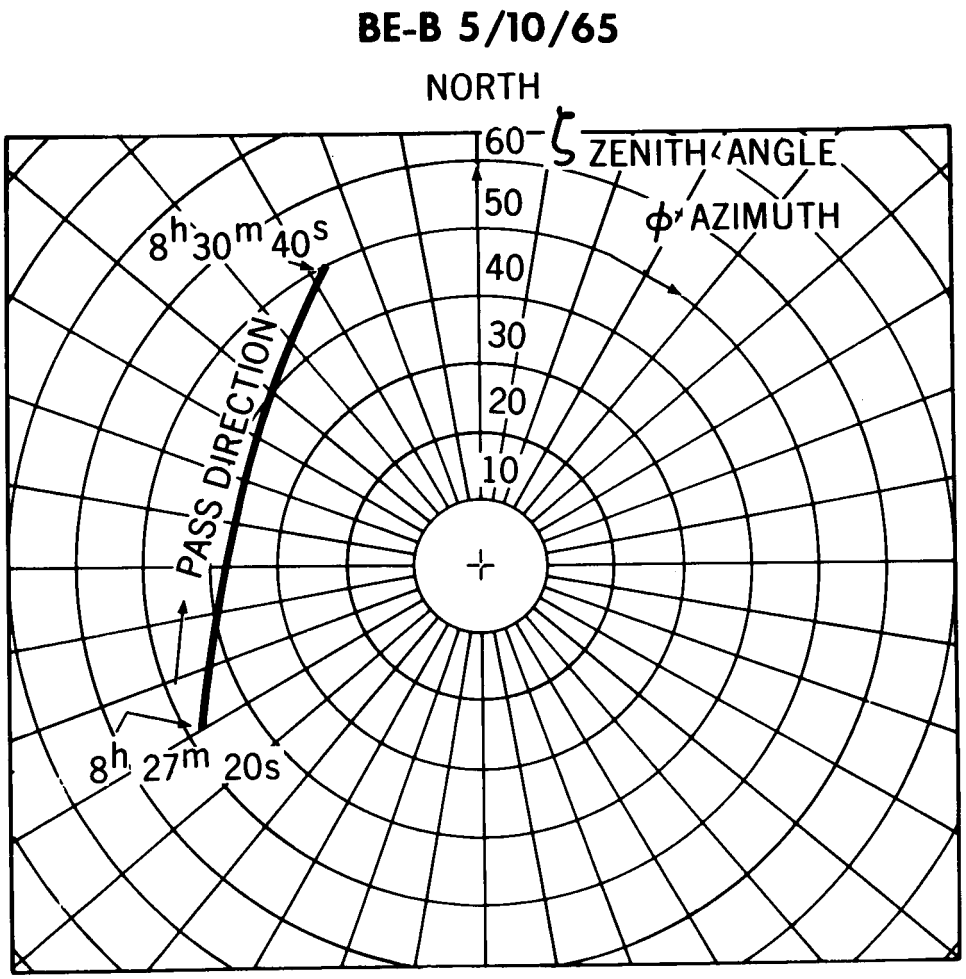

FIGURE 17. POLAR PLOT OF VISIBLE PORTION OF THE PASS OF EXPLORER 22 OVER GODDARD ON THE MORNING OF MAY 10, 1965.

To evaluate (16) in this case

$$\vec{R} \times \vec{\delta} = R_x \delta \vec{j} - R_y \delta \vec{k}$$

$$|\vec{R} \times \vec{\delta}| = \delta \left[R_y^2 + R_z^2 \right]^{1/2}$$

$$\alpha_s = \frac{R_x^2 \delta^2 - R^2 \delta^2}{R^2 \delta \left[R^2 - R_x^2 \right]^{1/2}}$$

$$= \frac{\delta}{R^2} \left[R^2 - R_x^2 \right]^{1/2} = \frac{\delta}{R} \left[1 - \sin^2 \varphi \cos^2 \varphi \right]^{1/2}$$

$$\alpha_s = 2\beta \left[1 - \sin^2 \varphi \cos^2 \varphi \right]^{1/2} \tag{26}$$

To evaluate α_N, we notice that $\vec{\delta}$ and $\vec{\ell}$ are in the same direction:

$$\vec{\gamma} = \vec{\delta} - \vec{\ell} = (\delta - \ell)\vec{\imath}$$

$$\vec{R} \times \vec{\gamma} = R_z (\delta - \ell)\vec{j} - R_y (\delta - \ell)\vec{k}$$

$$|\vec{R} \times \vec{\gamma}| = (\delta - \ell) \left[R_z^2 + R_y^2 \right]^{1/2} \tag{27}$$

(18) now becomes

$$\alpha_N = \frac{R_x^2 (\delta - \ell)^2 - R^2 (\delta - \ell)^2}{R^2 (\delta - \ell) \left[R_y^2 + R_z^2 \right]^{1/2}}$$

$$= \frac{(\delta - \ell)}{R^2} \left[R^2 - R_x^2 \right]^{1/2}$$

$$= \frac{\delta - \ell}{R} \left[1 - \sin^2 \varphi \cos^2 \varphi \right]^{1/2}$$

$$\alpha_N = \left(2\beta - \frac{\ell}{R} \right) \left[1 - \sin^2 \varphi \cos^2 \varphi \right]^{1/2} \tag{28}$$

(26) and (28) are the equations needed to analyze the BE-B pass of May 10, 1965.

A sufficient number of returns was received during this pass to produce the range vs. time plot in Figure 18. Figure 19 shows that the north receiving mount in this case received greater intensities because the reflected spot had been displaced to the north. Both figures thus appear to substantiate the effect of velocity aberration qualitatively. More thorough studies are continuing at this time.

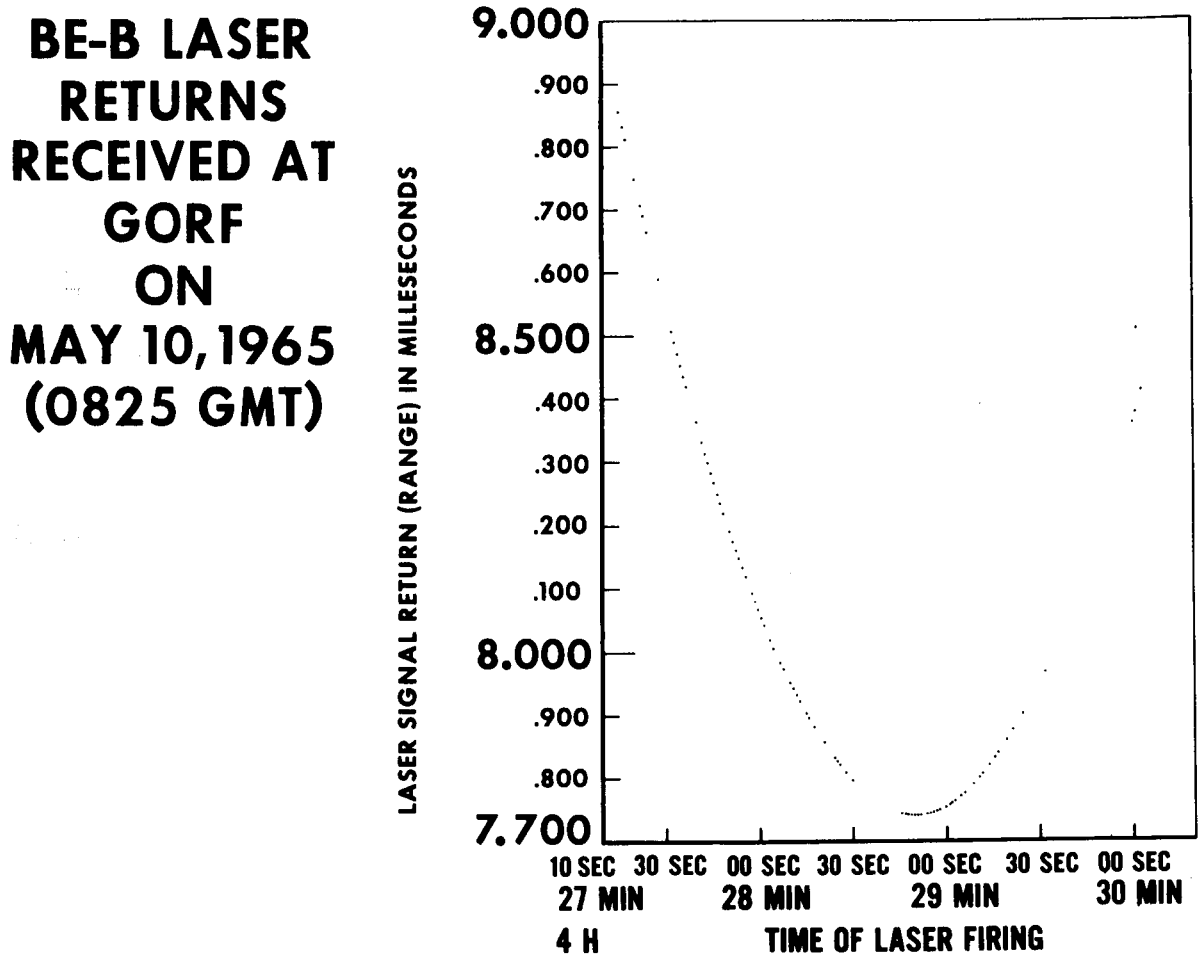

FIGURE 18. RANGE OF EXPLORER 22 AS DETERMINED BY LASER PULSE TIME OF FLIGHT MEASUREMENTS.

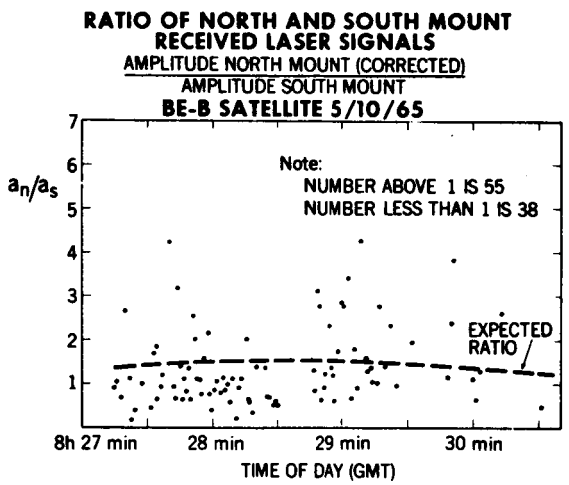

FIGURE 19.